JACS
JOURNAL OF THE AMERICAN CHEMICAL SOCIETY
Article
pubs.acs.org/JACS

Electrocatalytic $Z \rightarrow E$ Isomerization of Azobenzenes

Alexis Goulet-Hanssens,[†] Manuel Utecht,[‡] Dragos Mutruc,[†] Evgenii Titov,[‡] Jutta Schwarz,[†] Lutz Grubert,[†] David Bléger,[†] Peter Saalfrank,*[,‡] and Stefan Hecht*[,†]

[†]Department of Chemistry & IRIS Adlershof, Humboldt-Universität zu Berlin, Brook-Taylor-Strasse 2, 12489 Berlin, Germany
[‡]Theoretische Chemie, Institut für Chemie, Universität Potsdam, Karl-Liebknecht-Strasse 24-25, 14476 Potsdam-Golm, Germany

Supporting Information

ABSTRACT: A variety of azobenzenes were synthesized to study the behavior of their E and Z isomers upon electrochemical reduction. Our results show that the radical anion of the Z isomer is able to rapidly isomerize to the corresponding E configured counterpart with a dramatically enhanced rate as compared to the neutral species. Due to a subsequent electron transfer from the formed E radical anion to the neutral Z starting material the overall transformation is catalytic in electrons; i.e., a substoichiometric amount of reduced species can isomerize the entire mixture. This pathway greatly increases the efficiency of (photo)switching while also allowing one to reach photostationary state compositions that are not restricted to the spectral separation of the individual azobenzene isomers and their quantum yields. In addition, activating this radical isomerization pathway with photoelectron transfer agents allows us to override the intrinsic properties of an azobenzene species by triggering the reverse isomerization direction ($Z \rightarrow E$) by the same wavelength of light, which normally triggers $E \rightarrow Z$ isomerization. The behavior we report appears to be general, implying that the metastable isomer of a photoswitch can be isomerized to the more stable one catalytically upon reduction, permitting the optimization of azobenzene switching in new as well as indirect ways.

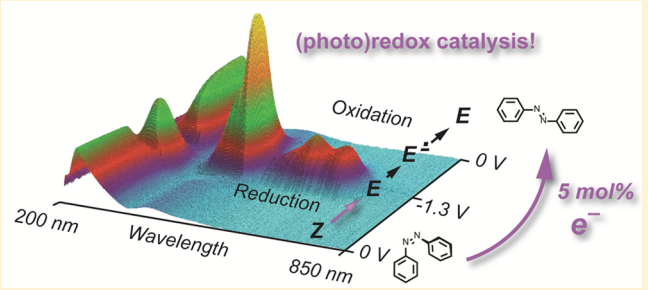

INTRODUCTION

Azobenzene continues to be one of the most widely used photochromic molecules due to the vastly different properties of its E and Z isomers and its ready availability, either commercially or by facile synthesis.[1−3] The isomerization around azobenzene's central N═N double bond drastically changes the geometry of the molecule, its polarity, and electronic properties.[4] Substitution on the aromatic rings affects many properties, including the absorption wavelength of both isomers and their photoisomerization quantum yield as well as the thermal half-life of the metastable Z isomer. As with most photoswitchable molecules, these properties are generally intrinsic to the molecules themselves.[5,6]

We were motivated to exploit the difference in the electronic levels of the two isomers of azobenzene,[7] following the successful use of other photoswitch families, such as diarylethenes[8,9] and spiropyrans,[10] in this context. Over the past half century, during which the reversible electrochemistry of azobenzene has been investigated,[11] generally two sequential one-electron reductions have been observed.[12] Neta and Levanon compared the radical anions derived from Z and E azobenzene spectroscopically and concluded that the same species were formed upon reduction, implying that there must be a mechanism for rapid $Z \rightarrow E$ isomerization from the Z azobenzene radical anion.[13] In agreement with this finding, Laviron and Mugnier observed no difference in the resulting two one-electron waves between the E and Z isomers at scan rates slower than 2 V/s;[14] however, higher scan rates and lower temperatures shifted the Z isomer's cathodic peak potential by +60 mV relative to the E isomer. In protic solvents, there is an additional pH dependence, with identical cathodic half-wave potentials of the E and Z isomers at pH < 11, and a +180 mV shift in the half-wave potential of the Z isomer at pH > 11.[15] The gaps between the cathodic peak potentials of the Z and E isomers in protic environments are highly dependent on the nature of the solvent used and range from +50 mV at pH 7 in 10% ethanol buffer[16] to over +120 mV in neat ethanol[17] to +200 mV in aqueous dioxane.[18] On the basis of these principles, Fujishima and co-workers developed a memory device using Langmuir−Blodgett films of an azobenzene derivative on an indium tin oxide transparent electrode, at which point after writing with light the formed Z isomer could selectively be reduced to the corresponding hydrazo compound due to a +400 mV shift in potential as compared to the E isomer in the aqueous environment.[19]

Photomodulated voltammetry (PMV) enabled Grampp and co-workers to distinguish the reduction potentials of the two azobenzene isomers, as they observed a cathodic shift of the reduction potential by −60 mV for the Z isomer in DMF.[20] The authors suggested that the use of PMV allowed for this observation as the technique is better suited to measure the

Received: October 16, 2016
Published: December 20, 2016

DOI: 10.1021/jacs.6b10822
J. Am. Chem. Soc. 2017, 139, 335−341

potential of short-lived species and postulated that the *Z* azobenzene radical anion rapidly isomerizes to the corresponding *E* radical anion, resulting in only the *E* isomer potential being measured in conventional cyclovoltammetry (CV) experiments.

Over the past three decades, diarylethenes (DAEs) have emerged as complementary and very versatile photochromic compounds.[21,22] DAEs have also been switched electrochemically as demonstrated for the first time by Branda and coworkers, reporting both oxidatively induced electrocyclic ring-opening[23] and ring-closing.[24] The direction of electrochemically induced switching depends on the relative thermodynamic stability of the two isomers, with oxidation of the metastable species serving as an alternative to optical excitation for triggering isomerization. Importantly, the ring-opening was shown by Branda to be a catalytic process,[23] in which the ring-opened radical cation oxidizes a second ring-closed molecule to propagate the reaction. This process has been initiated through electrocatalysis, through direct oxidation, or through photoelectrocatalysis[25] using photoelectron transfer agents to oxidize the ring-closed DAE and initiate the catalytic cycle.[26] Similar catalysis has been shown in dithiazolythiazoles, where the current efficiency was calculated to be as high as 900%.[27] In parallel and seemingly unrelated work, increased thermal $Z \rightarrow E$ isomerization rates of azobenzenes in the presence of nanoparticles have been reported. Depending on the nature of the azobenzene and the surface functionalization of the nanoparticles, up to 40 molecules of azobenzene could be quantitatively isomerized from the *Z* to the *E* isomer,[28] and the observed rate acceleration was quantified to be between 1 and 6 orders of magnitude.[29] The exact mechanism of the enhanced thermal $Z \rightarrow E$ isomerization of azobenzene on a (flat or curved) gold surface was explored theoretically and experimentally, and the authors suggested that an electron transfer from the azobenzene to the nanoparticle was the preferred reaction pathway.[30] The resulting azobenzene radical cation was postulated to have a much shorter thermal half-life.

Here we detail a comprehensive investigation of the electrocatalytic switching of azobenzenes and show that it is a general phenomenon. For this purpose we studied the electrochemistry of more than a dozen different azobenzene derivatives, which all exhibit identical cathodic peak potentials of both their *E* and *Z* isomers due to rapid isomerization of the *Z* azobenzene radical anion. To access the elusive *Z* isomer radical anion, we prepared a cyclic derivative, in which $Z \rightarrow E$ isomerization is geometrically prohibited, and observed the expected higher cathodic peak potential relative to its *E* isomer. From spectroelectrochemical studies we derived a mechanistic model to rationalize the catalytic $Z \rightarrow E$ isomerization upon electrochemical reduction. This reduction of the *Z* isomer takes place at absolute potentials smaller than that necessary for reduction of the *E* isomer, although we demonstrate that the *Z* isomer's LUMO level is in fact higher in energy than the *E* isomer's LUMO level. However, relaxed electron affinities calculated by means of the ΔSCF approach suggest that there is almost no difference between *Z* and *E* isomers. Anyway, the reason for this unusual behavior is the tremendously accelerated thermal $Z \rightarrow E$ isomerization of the radical anion as compared to that of the neutral azobenzene. Chain propagation via electron transfer from the *E* isomer radical anion to the *Z* isomer allows one to rapidly isomerize a solution of *Z* azobenzene with a substoichiometric amount of electrons (Figure 1).

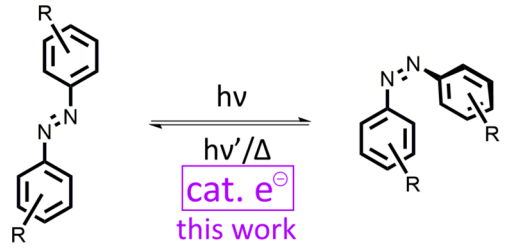

Figure 1. Light induces $E \rightarrow Z$ isomerization of azobenzene while an alternative wavelength of light or heat triggers the reverse isomerization. In this work we show that efficient and quantitative $Z \rightarrow E$ isomerization can be triggered by a catalytic amount of electrons, which can be supplied directly or indirectly with the aid of a photoelectron transfer agent.

In addition, we demonstrate the use of photoelectron transfer agents to induce this catalytic isomerization. The use of this alternative pathway, as opposed to direct azobenzene excitation, opens the door to tune the wavelength required for isomerization and to render the quantum yield independent from chemical functionalization of the azobenzene itself. We show that one can even override the isomerization preference at a given wavelength, obtaining *E* enriched photostationary states (PSS) at wavelengths that would typically provide *Z* enriched PSS mixtures.

RESULTS AND DISCUSSION

Reduction Potential of *E* and *Z* Azobenzenes. Upon conversion of the flat and fully π-conjugated *E* isomer to the twisted *Z* isomer, the extent of π-conjugation is reduced, leading to a shift of both the HOMO (n) and LUMO (π*) levels to higher energies as confirmed computationally.[7,31] For the parent azobenzene **1**, the LUMO energy of the *E* isomer is calculated to be −2.77 eV, being 0.27 eV lower as compared to the *Z* isomer with E_{LUMO} = −2.50 eV (see Table S7 in the Supporting Information, calculated with B3LYP/6-311++G**, solvent corrected for acetonitrile using the polarizable continuum model). However, taking relaxed ΔSCF electron affinities, we find almost no difference between *Z* and *E* isomers in their tendency to accept an electron (see Table S7). In agreement with these findings, our voltammetry experiments employing a rotating ring-disc electrode (RRDE) yielded the same results for both isomers (Figure 2), suggesting that the cathodic peak potential as well as the kinetic stability of the radical anion derived from the *Z* isomer and the *E* isomer are in fact identical.

Another possible explanation for equal peak potentials could be that a very efficient conversion of the *Z* to the *E* isomer is induced upon reduction to the radical anion. To test this theory, we designed the cyclic azobenzene derivative **3**, in which the *Z* configuration is locked (see molecular structure determined by single crystal X-ray diffraction, Figure S25 in the Supporting Information) and compared it to its linear analogue **2** that is able to interconvert between its *E* and *Z* isomers, *E*-**2** and *Z*-**2**, respectively (Figure 3, top). Optical spectra in a variety of solvents and over a temperature range from −100 to 100 °C verify that locked azobenzene *Z*-**3** indeed does not undergo any detectable thermal or photoinduced isomerization (see Figure S24 in the Supporting Information). Subsequent cyclic voltammetry experiments of azobenzene **2** (Figure 3, bottom) resemble the ones conducted with the parent azobenzene **1**; i.e., the reduction of the *E* and *Z* isomers

DOI: 10.1021/jacs.6b10822
J. Am. Chem. Soc. 2017, 139, 335−341

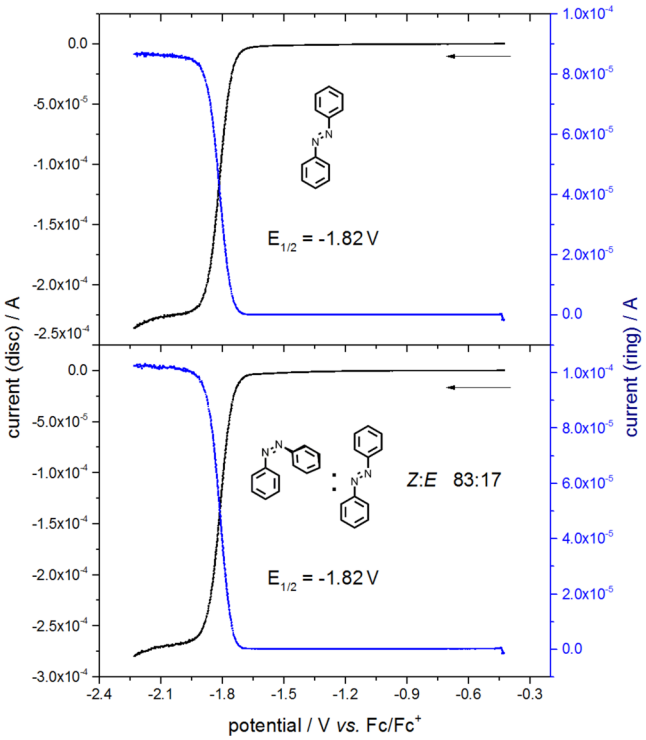

Figure 2. Voltammetry of unsubstituted *E* azobenzene *E*-**1** (top) and *Z* azobenzene *Z*-**1** (as the PSS mixture containing 83% *Z*-**1**, bottom) with a rotating glassy-carbon ring-disc electrode, showing identical cathodic peak potentials of the *E* and *Z* isomers and a comparable stability of the formed radical anion species. Instrument details: r_1 = 2.850 cm; r_2 = 3.125 cm; r_3 = 3.975 cm, N_0 = 0.398, rotation = 1000 rpm, [**1**] = 5×10^{-4} M in 0.1 M Bu_4NPF_6 acetonitrile solution.

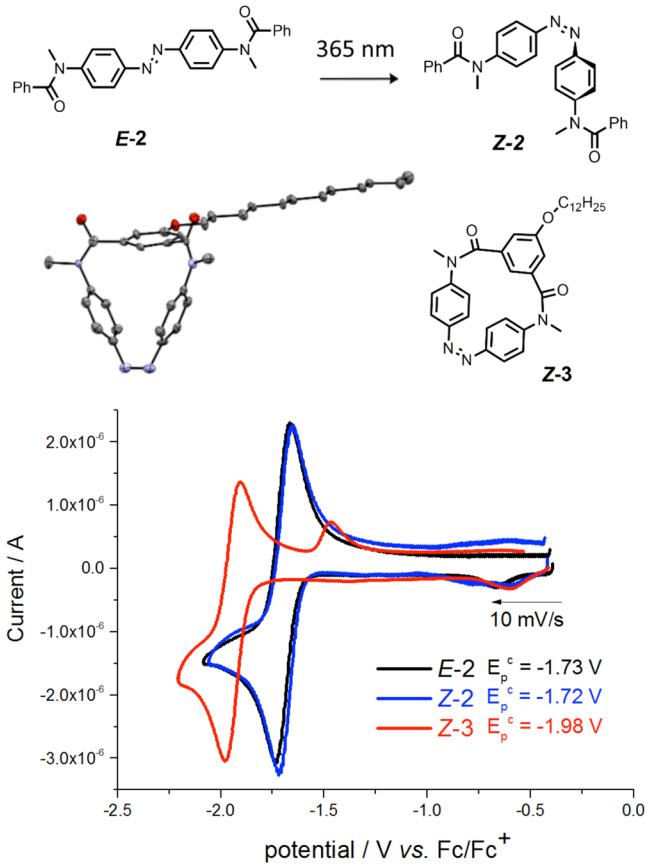

Figure 3. Chemical structures of the two isomers of azobenzene derivative **2** (top). A *Z*-enriched mixture containing 81% of *Z*-**2** is obtained by irradiating *E*-**2** with 365 nm light. The cyclic azobenzene analogue **3**, which is locked as the *Z* isomer (middle, single crystal X-ray diffraction structure shown as ORTEP plot with 50% probability ellipsoids), and corresponding cyclic voltammograms in acetonitrile (bottom), showing a 250 mV higher reduction potential of *Z*-**3** as compared to *E*-**2** and *Z*-**2**, which are identical.

occurs at the same potential of $E_p^c = -1.73$ V (all potentials are reported vs Fc/Fc^+). In the case of the cyclic azobenzene *Z*-**3**, a reduction potential that is 250 mV more negative than the cathodic peak potential of the linear isomers was measured. Computations place the LUMO of the *Z*-**3** at −2.31 eV compared to −2.62 eV for *Z*-**2**, both of which are higher than the LUMO level of the *E*-**2** isomer at −2.84 eV. Therefore, we assign the measured cathodic peak potential in the case of *Z*-**3** to correspond to the LUMO level of the *Z* isomer, which in the case of linear analogue **2**, and most other azobenzene derivatives, is not accessible experimentally. Although the reduction *Z*-**3** is reversible, the anodic wave in the CV at −1.4 V is indicative of a subsequent reaction of the radical anion.

Spectroelectrochemistry of *E* and *Z* Azobenzene. The clearly distinct cathodic peak potentials of the electronically rather similar *Z* azobenzenes *Z*-**2** and *Z*-**3** indeed support a chemical transformation triggered during the course of the electrochemical measurement in the case of *Z*-**2**. Using an additional method such as optical absorption spectroscopy during the cyclovoltammetry measurement allows for the observation of each species generated in the course of the overall reduction−oxidation process from the neutral azobenzene to the radical anion and back to the neutral azobenzene. Azobenzene derivative **4** was selected for this study due to the greatly enhanced thermal half-lives of *ortho*-fluorinated *Z* azobenzenes at room temperature and the high *Z* isomer content of 90% in the photostationary state (PSS) upon irradiation above 500 nm.[31,32] A slow reduction process was initiated at a speed of 10 mV/s, and the corresponding UV−vis spectra were recorded every 10 mV. The potential was measured from 0.22 to −1.52 V and back to 0.22 V giving rise to a total of 301 spectra (see Figures S33 and S34 of the Supporting Information). Upon an increase of the (absolute value of the) reductive potential the spectra show a strong decrease in the absorbance of the initial $\pi \rightarrow \pi^*$ transition of *E*-**4** and emergence of new bathochromically shifted bands at 493, 625, and 691 nm attributed to the formed radical anion of *E*-**4**. This assignment is based on the similarity with spectra of previously reported azobenzene anion radicals[33] and the fact that exactly 1 equiv of electrons was transferred at the maximum absorbance and hence reflects the concentration of the formed species as measured by coulometry. Since the reduction is fully reversible, the final spectrum after cyclic voltammetry is identical to the initial spectrum of *E*-**4**.

The same spectroelectrochemical experiment was carried out with a solution of azobenzene **4**, irradiated to its PSS containing 90% *Z*-**4** (Figure 4, top). Already at a potential of −0.91 V, clearly before reaching the onset of the reduction peak, the spectrum undergoes a dramatic change characterized by a sharp increase in the $\pi \rightarrow \pi^*$ band with a concomitant decrease of the $n \rightarrow \pi^*$ transition. These spectral changes clearly show that *Z* → *E* isomerization is occurring before the reduction to the radical anion is actually taking place. In contrast to the formation of the radical anion, where 1 equiv of electrons is

DOI: 10.1021/jacs.6b10822
J. Am. Chem. Soc. 2017, 139, 335−341

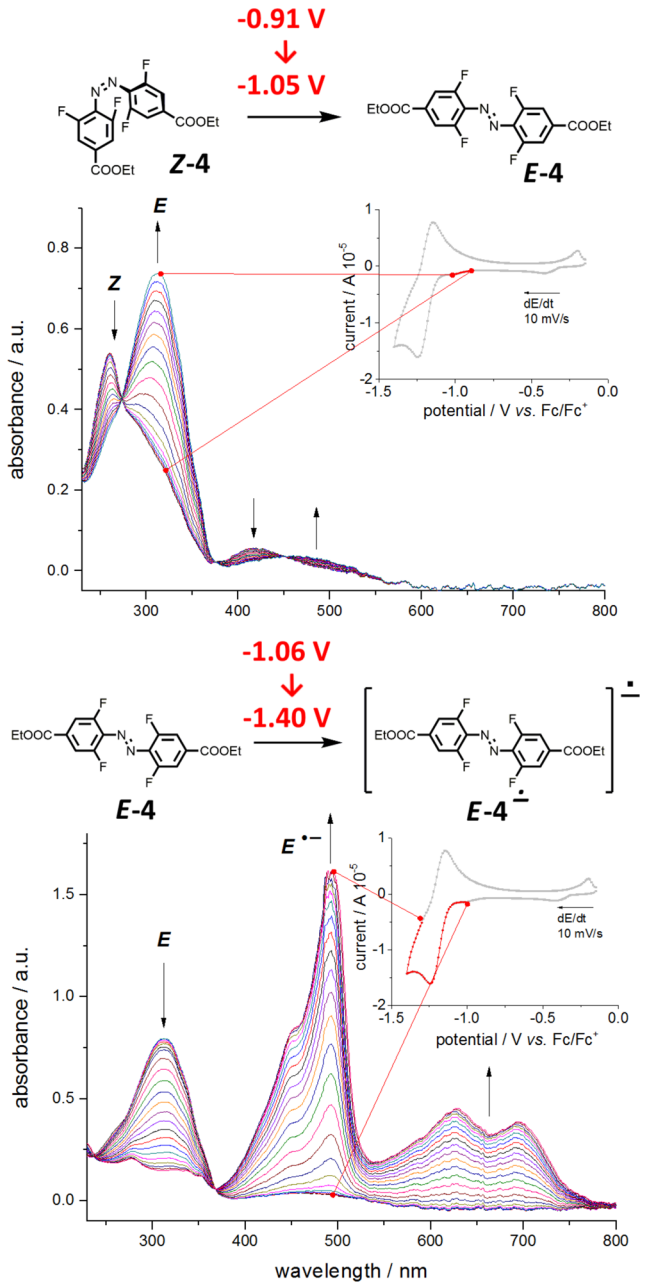

Figure 4. UV−vis spectral changes during cyclovoltammetry of *Z*-**4**: Initial and efficient $Z \rightarrow E$ isomerization in the range from −0.91 to −1.05 V (top) followed by generation of the *E*-**4** radical anion in the range from −1.06 to −1.40 and back to −1.30 V (bottom). All spectra were acquired in a 1 mm quartz cuvette, with Pt electrodes in the presence of 0.1 M Bu_4NPF_6. $c = 5 \times 10^{-4}$ M, Pt electrode, −0.15 V → −1.30 V → −0.15 V, dE/dt =10 mV/s.

necessary to transform the bulk solution, the initial $Z \rightarrow E$ isomerization requires far less than 1 equiv of electrons as judged by the negligible current of 1.4 μA (see Figure 4, top). Subsequent further increase of the reductive potential leads to formation of the radical anion of *E*-**4** (Figure 4, bottom) showing that the involved species over the entire potential range are identical to the ones observed in the direct reduction of *E*-**4** as described above (see also Figure S34 in the Supporting Information). In both cases, the species recovered after a full reduction−oxidation cycle is the *E* isomer.

In our studies, we investigated 13 different azobenzene derivatives (Table S2), both as their pure *E* isomers and the *Z*-rich PSS mixtures, and all compounds showed a similar $Z \rightarrow E$ isomerization event occurring approximately 150−350 mV before the cathodic peak potential, corresponding to the radical anion of the *E* isomer (the onset of this isomerization is tabulated in Table S5). At the employed scan rate (10 mV/s) there is a negligible amount of isomerization before the electrochemically induced event. Note that thermal isomerization can be excluded as we studied several fluorinated azobenzenes with thermal half-lifes of up to 2 years.[31] In addition to dramatically increasing the thermal half-life,[32] fluorine substitution strongly affects the cathodic peak potential, which was measured between −1.18 and −2.00 V (see section 4.16 in the Supporting Information). Importantly, in all of the investigated derivatives, the acceleration of the $Z \rightarrow E$ isomerization was similar, indicating that it is independent of the cathodic peak potential.

In view of our results, the reductively induced $Z \rightarrow E$ isomerization process seems to be general, and because only a small amount of current is flowing through the sample during the reaction, it cannot be stoichiometric in electrons. Integrating the region of the cyclic voltammogram where the $Z \rightarrow E$ isomerization takes place yields a current only approximately 5% of the value required to reduce the entire amount of azobenzene present in solution to the radical anion. Therefore, this experiment for the first time provides direct evidence that the $Z \rightarrow E$ isomerization is indeed electrocatalytic,[34] as has been suggested in previous literature reports,[14,20] and as a result explains why direct measurement of the *Z* isomer's cathodic peak potential using standard electrochemical techniques is not feasible. The fact, however, that the isomerization event occurs anodically shifted from where computation and our experiments with the locked *Z* azobenzene **3** suggesting that the cathodic peak potential of the *Z* isomer should occur can be explained with the aid of Nernst's equation (eq 1):

$$E_{1/2} = E^\circ + \frac{RT}{zF}\ln\left(\frac{a_{ox}}{a_{red}}\right) \quad (1)$$

According to this equation, the half-wave electrode potential ($E_{1/2}$) of a given redox process (involving *z* electrons at a given temperature *T*) depends on the standard potential (E°) and the ratio of the activity coefficients of the two involved redox-active species (a_{ox} and a_{red}). In the case of a fully reversible redox process, the second term vanishes since $a_{ox} = a_{red}$ and hence $E_{1/2} = E^\circ$. Indeed, for *E* azobenzene, the half-wave electrode potential equals the standard potential. In the case of the reduction of *Z* azobenzene, however, the formed *Z* radical anion undergoes rapid $Z \rightarrow E$ isomerization; hence, the concentration of this species is constantly depleted, and the system is pulled out of equilibrium such that $E_{1/2} \neq E^\circ$. As a result, positive shifts of $E_{1/2}$ relative to E° are observed, which in the investigated derivatives range between 150 and 350 mV, corresponding to ratios of the neutral *Z* isomer and its corresponding radical anion (a_{ox}:a_{red}) in the order of 340:1 to 830 000:1. This shift explains why the formation of the *Z* radical anion occurs prior to reaching the cathodic peak potential, which is required to form the *E* radical anion.

From these data we postulate the mechanism sketched in Figure 5 (left), which explains why the reduction process is catalytic once the *Z* azobenzene radical anion ($Z^{\bullet-}$) enters the

DOI: 10.1021/jacs.6b10822
J. Am. Chem. Soc. 2017, 139, 335−341

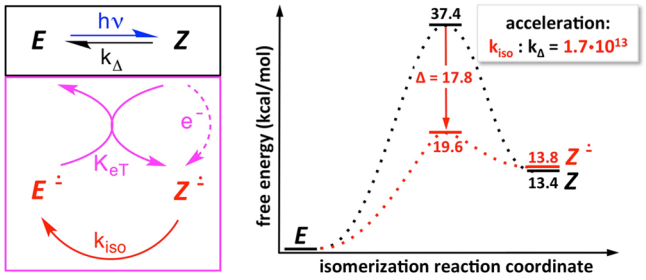

Figure 5. Proposed mechanism and reason for observed rate acceleration: Upon initial azobenzene photoisomerization (blue arrow), the formed Z isomer can undergo thermal $Z \rightarrow E$ isomerization either via its neutral form (black box) or via its radical anion (magenta box). The latter pathway involves a radical chain reaction, which after initial reduction using catalytic amounts of electrons to form the radical anion $Z^{\bullet-}$ involving rapid isomerization to $E^{\bullet-}$ (red arrow) followed by an electron transfer equilibrium (magenta arrows) to yield the neutral E product and regenerate $Z^{\bullet-}$ to propagate the chain. The thermoneutral electron transfer equilibrium (K_{eT}) is driven by the extremely rapid and irreversible isomerization step (k_{iso}), which in the case of azobenzene at room temperature has been calculated to be accelerated by 13 orders of magnitude as compared with that of neutral $Z \rightarrow E$ isomerization (right).

cycle. Upon initiation by reducing a small amount of Z isomer, the formed $Z^{\bullet-}$ isomerizes extremely rapidly to the radical anion of the E isomer ($E^{\bullet-}$),[13,14] which subsequently transfers an electron to another neutral Z isomer to propagate the cycle. The calculated electron affinities (see Table S7 in the Supporting Information) suggest that the electron transfer equilibrium (K_{eT}) between the azobenzene isomers and specifically from $E^{\bullet-}$ to substrate Z to yield $Z^{\bullet-}$ and product E is almost thermoneutral. The subsequent removal of $Z^{\bullet-}$ via rapid and irreversible isomerization (k_{iso}) to the thermodynamically favored E isomer drives the equilibrium to the product side.

In order to rationalize the origin of the fast thermal $Z \rightarrow E$ isomerization taking place in the radical anion, the activation barriers for both the charge-neutral azobenzene as well as the corresponding radical anion were evaluated computationally (Figure 5, right). While the thermodynamic driving force for $Z \rightarrow E$ isomerization is nearly identical in both cases, i.e., $\Delta G(Z \rightarrow E)$ = 13.4 kcal/mol versus $\Delta G(Z^{\bullet-} \rightarrow E^{\bullet-})$ = 13.8 kcal/mol, the energy of the transition state in the case of the radical anion isomerization ($\Delta G^{\ddagger}$ = 19.6 kcal/mol) is much lower as compared to the charge-neutral case ($\Delta G^{\ddagger}$ = 37.4 kcal/mol). This tremendously decreased thermal barrier in the case of the radical anion leads to a dramatic rate enhancement by 13 (!) orders of magnitude at 298.15 K, i.e., from $k_{\Delta} = 1.9 \times 10^{-5}$ s^{-1} to $k_{iso} = 3.3 \times 10^{8}$ s^{-1}. This calculated rate acceleration is in qualitative agreement with the experimental 6 orders of magnitude increase measured by Zhao and co-workers for electric field enhanced $Z \rightarrow E$ isomerization in azobenzene liquid crystals[35] as well as the 2 orders of magnitude increase seen by Enomoto and co-workers in Langmuir–Blodgett films,[36] with both studies conducted in the absence of an electrolyte. In previous work by our own and the Grill group, we could show that, at very low temperatures of 7 K and in ultrahigh vacuum, azobenzene $Z \rightarrow E$ isomerization could only occur in the junction of the scanning tunneling microscope, implying a significant reduction of the isomerization barrier under the influence of a strong electric field.[37−39] Computations were performed with B3LYP/6-311++G** ((for full computational details see section 6 of the Supporting Information, and for results see Table S8).

Photoelectrocatalytic Switching. On the basis of the above electrocatalytic switching mechanism, we were interested in exploiting indirect excitation to induce the $Z \rightarrow E$ isomerization.[5,40] We selected an iridium complex, *fac*-tris(2-(3-*p*-xylyl)phenyl)pyridine iridium(III) (Ir(dmpppy)$_3$)), known to be an efficient photoelectron transfer agent,[41] since its LUMO energy level is higher in energy than that of azobenzene providing the thermodynamic driving force for efficient photoelectron transfer. We investigated the parent azobenzene **1**, which was irradiated at 365 nm to its Z-rich PSS containing 83% of Z-**1**, before the iridium complex was added and the solution was degassed. In the absence of any Ir(dmpppy)$_3$, upon irradiation with light of 365 nm, the PSS remains unaffected and contains 17% E-**1** (Figure 6). In

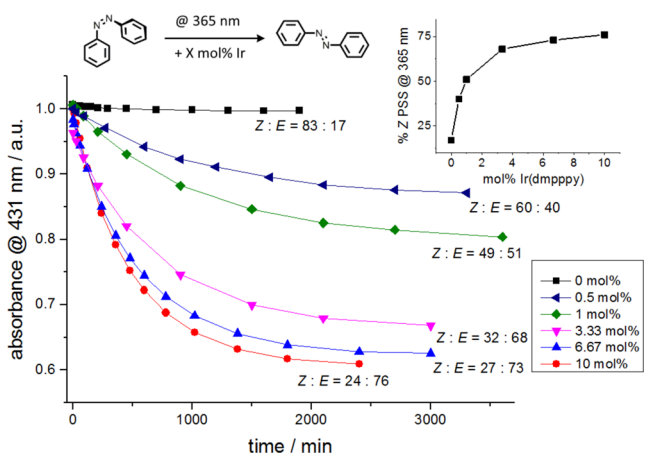

Figure 6. Catalytic reductive $Z \rightarrow E$ isomerization of parent azobenzene **1** triggered by photoinduced electron transfer from an iridium complex (Ir(dmpppy)$_3$): Upon addition of catalytic amounts of Ir(dmpppy)$_3$ to the Z-rich PSS mixture (containing 83% of Z-**1**) and subsequent irradiation at 365 nm, the amount of E isomer in the PSS is substantially improved (inset, top right) while also the isomerization rate is dramatically increased.

contrast, with the addition of only 0.5 mol % of Ir(dmpppy)$_3$ this yield increases to 40% E-**1**. Increasing the iridium to the azobenzene ratio leads to a concomitant increase in the E content of the PSS (Figure 6, inset) until a saturation limit is reached, as in our experiments an increase of 6.67 to 10 mol % Ir(dmpppy)$_3$ led to only a slight improvement in the PSS. The observed concentration dependence supports a photoinduced electron transfer from the excited Ir(dmpppy)$_3$ complex to the Z azobenzene thereby forming the Z azobenzene radical anion and initiating the catalytic cycle.

The extent of photochemically induced switching that can be achieved in a photochromic system is described by the PSS at a specific irradiation wavelength. Typically, only direct excitation is being considered, and hence, the PSS is defined by the ratio of the extinction coefficients of the two interconverting isomers and the ratio of the quantum yields for the forward and backward reactions, all at the employed irradiation wavelength. In our case, however, we have to furthermore consider indirect excitation via the iridium complex. The efficiency of initiating the radical chain is governed by the kinetics of the photoinduced electron transfer from the excited iridium complex to the Z isomer. Therefore, the overall composition

DOI: 10.1021/jacs.6b10822
J. Am. Chem. Soc. 2017, 139, 335−341

of the PSS should be given by eq 2 (derived in section 5.1 of the Supporting Information):

$$\frac{[E]_{PSS}}{[Z]_{PSS}} = \frac{\varepsilon_Z^{\lambda}\varphi_{Z\to E}}{\varepsilon_E^{\lambda}\varphi_{E\to Z}} + \frac{[Ir^*]_{PSS}k_2}{\varepsilon_E^{\lambda}\varphi_{E\to Z}} \quad (2)$$

In the case of azobenzene **1**, when we irradiate with 365 nm light, where the *E* isomer absorbs preferentially, the PSS becomes enriched in *Z* isomer (83% *Z*-**1**) as dictated by the first (left) term shown in black on the right side of eq 2. However, upon addition of an appropriate photoelectron transfer agent, i.e., the iridium complex, an additional second (right) term on the right side of eq 2 becomes increasingly important. In fact, this indirect excitation pathway drives the photoreaction in the opposite direction (and can only drive it in the $Z \rightarrow E$ direction!) of the direct excitation route and allows one to override the intrinsic photochromic behavior of the switch in a tunable fashion. Importantly, in such sensitized systems the ratio of *E* and *Z* azobenzene can be constantly varied as a function of the iridium concentration, and hence, we could successfully overcome the boundaries of a conventional photostationary state, i.e., not being limited by intrinsic quantum yields and absorption spectra of the azobenzene isomers!

Our system is closely related to photoredox catalytic systems in the literature,[42−44] where photoexcitation of a catalyst (typically, but not necessarily a transition metal complex) drives electron transfer to activate the substrate, which subsequently undergoes a particular chemical transformation after which the catalyst is regenerated by back electron transfer. While the term photoredox catalysis relates to the catalytically active species being present in substoichiometric amounts, the process itself is not necessarily catalytic in electrons.[34] In our case, however, the iridium complex is present in catalytic amounts, and the product of the initial photoinduced electron transfer, i.e., the radical anion, itself becomes the catalyst. Formation of $Z^{\bullet-}$ followed by immediate isomerization provides $E^{\bullet-}$, from which there is an inherent competition between the propagation of the catalytic chain (involving electron transfer to another neutral *Z* isomer) or back electron transfer to the formed oxidized Ir(IV) complex. This competition is reflected in the saturation behavior with increasing concentration of the iridium complex (see inset in Figure 6).

Last but not least, we want to point out that our system certainly could be improved. For example, we were not able to identify a suitable photoelectron transfer agent with an absorption wavelength completely separated from the azobenzene absorption. The overlapping spectra (see Figure S61 in the Supporting Information) are the reason why our attainable PSS is limited to 76% *E* isomer. Although the photoredox catalysis is highly efficient, as demonstrated by more than doubling the *E* content with as little as 0.5 mol % iridium complex, even at an amount of 10 mol % iridium direct absorption of approximately one-fifth of the photons by the azobenzene prevents quantitative $Z \rightarrow E$ isomerization.

CONCLUSION

We have investigated the electrochemistry of a variety of azobenzene derivatives as their *E* and *Z* isomers. In all examples we found rapid thermal $Z \rightarrow E$ isomerization, which can be induced reductively by a catalytic amount of electrons. This isomerization process is independent of thermal half-life and cathodic peak potential and occurs before reaching the cathodic peak potential of the *E* isomer. This overall catalytic process is enabled by the dramatically accelerated isomerization on the radical anion potential energy surface; i.e., $Z^{\bullet-} \rightarrow E^{\bullet-}$ is 10^{13} times faster than $Z \rightarrow E$, and driven by the buildup of the thermodynamically more stable *E* isomer.

Our work clarifies the mechanism and generality of previous observations regarding the electrochemical switching of *Z* azobenzenes,[13,20] and follows similar observations of electrochemical switching in diarylethenes,[23,26,27] stilbenes,[45,46] and thioindigos.[47,48] Through the use of computational methods, we elucidate that the potential energy surface of the radical anion allows for a dramatic increase in the rate of thermal $Z \rightarrow E$ isomerization. As opposed to the reductive ring-closing observed in some fulgides,[49] the observed isomerization is catalytic. We are convinced that in many families of photoswitches this phenomenon is general and currently underexploited. For example by initiating this electrocatalytic switching process using an iridium complex as a photoelectron transfer agent, azobenzenes can conveniently be isomerized via indirect excitation. Such coupled systems provide photostationary states that are no longer solely dependent on the isomerization quantum yields and extinction coefficients of the individual isomers of azobenzene (or another photoswitch), but instead can be tuned by adjusting the concentration of the photoelectron transfer agent. Using this new blend of photochromism and photoredoxcatalysis opens the door to more efficient and orthogonal remote control over functional molecular systems, materials, and devices with light.

ASSOCIATED CONTENT

Supporting Information

The Supporting Information is available free of charge on the ACS Publications website at DOI: 10.1021/jacs.6b10822.

Synthetic details and ^{1}H and ^{13}C NMR spectra of new compounds, spectroelectrochemistry, and computational details (PDF)

Crystallographic details (CIF)

AUTHOR INFORMATION

Corresponding Authors

*petsaal@uni-potsdam.de

*sh@chemie.hu-berlin.de

ORCID

Evgenii Titov: 0000-0002-1732-1826

Stefan Hecht: 0000-0002-6124-0222

Notes

The authors declare no competing financial interest.

ACKNOWLEDGMENTS

We are grateful to our dedicated co-workers and collaborators, who have contributed to our own research endeavor in this field over the past years. A.G.-H. is indebted to the Alexander von Humboldt-Foundation and the FQRNT for providing postdoctoral fellowships. Generous support from the Daimler Benz-Foundation (via 32-02/14) as well as the European Research Council (via ERC-2012-StG_308117 "Light4Function") is gratefully acknowledged. D.B. acknowledges the German Research Foundation (DFG via BL 1269/1).

DOI: 10.1021/jacs.6b10822
J. Am. Chem. Soc. 2017, 139, 335−341

REFERENCES

(1) Beharry, A. A.; Woolley, G. A. *Chem. Soc. Rev.* **2011**, *40*, 4422−4437.
(2) Merino, E. *Chem. Soc. Rev.* **2011**, *40*, 3835−3853.
(3) Mahimwalla, Z.; Yager, K. G.; Mamiya, J.; Shishido, A.; Priimagi, A.; Barrett, C. J. *Polym. Bull.* **2012**, *69*, 967−1006.
(4) Bandara, H. M. D.; Burdette, S. C. *Chem. Soc. Rev.* **2012**, *41*, 1809−1825.
(5) Bléger, D.; Hecht, S. *Angew. Chem., Int. Ed.* **2015**, *54*, 11338−11349.
(6) *Molecular Switches*, 2nd ed.; Feringa, B. L., Browne, W. R., Eds.; Wiley-VCH Verlag GmbH: Weinheim, Germany, 2011.
(7) Del Valle, M.; Gutiérrez, R.; Tejedor, C.; Cuniberti, G. *Nat. Nanotechnol.* **2007**, *2*, 176−179.
(8) Gemayel, M. El; Börjesson, K.; Herder, M.; Duong, D. T.; Hutchison, J. A.; Ruzié, C.; Schweicher, G.; Salleo, A.; Geerts, Y.; Hecht, S.; Orgiu, E.; Samorì, P. *Nat. Commun.* **2015**, *6*, 6330.
(9) Leydecker, T.; Herder, M.; Pavlica, E.; Bratina, G.; Hecht, S.; Orgiu, E.; Samorì, P. *Nat. Nanotechnol.* **2016**, *11*, 769−775.
(10) Suda, M.; Kato, R.; Yamamoto, H. M. *Science* **2015**, *347*, 743−746.
(11) Sadler, J. L.; Bard, A. J. *J. Am. Chem. Soc.* **1968**, *90*, 1979−1989.
(12) Stradins, J. P.; Glezer, V. T. In *Encyclopedia of Electrochemistry of the Elements, Volume XIII*; Bard, A. J., Lund, H., Eds.; Dekker: New York, 1979; p 163.
(13) Neta, P.; Levanon, H. *J. Phys. Chem.* **1977**, *81*, 2288−2292.
(14) Laviron, E.; Mugnier, Y. *J. Electroanal. Chem. Interfacial Electrochem.* **1978**, *93*, 69−73.
(15) Laviron, E.; Mugnier, Y. *J. Electroanal. Chem. Interfacial Electrochem.* **1980**, *111*, 337−344.
(16) Gupta, P. N.; Raina, A. *J. Indian Chem. Soc.* **1988**, *65*, 495−497.
(17) Compton, R. G.; Wellington, R. G.; et al. *J. Electroanal. Chem.* **1992**, *322*, 183−190.
(18) Klopman, G.; Doddapaneni, N. *J. Phys. Chem.* **1974**, *78*, 1825−1828.
(19) Liu, Z. F.; Hashimoto, K.; Fujishima, A. *Nature* **1990**, *347*, 658−660.
(20) Grampp, G.; Mureşanu, C.; Landgraf, S. *J. Electroanal. Chem.* **2005**, *582*, 171−178.
(21) Irie, M. *Chem. Rev.* **2000**, *100*, 1685−1716.
(22) Irie, M.; Fukaminato, T.; Matsuda, K.; Kobatake, S. *Chem. Rev.* **2014**, *114*, 12174−12277.
(23) Peters, A.; Branda, N. R. *J. Am. Chem. Soc.* **2003**, *125*, 3404−3405.
(24) Peters, A.; Branda, N. R. *Chem. Commun.* **2003**, 954−955.
(25) Lee, S.; You, Y.; Ohkubo, K.; Fukuzumi, S.; Nam, W. *Angew. Chem., Int. Ed.* **2012**, *51*, 13154−13158.
(26) Lee, S.; You, Y.; Ohkubo, K.; Fukuzumi, S.; Nam, W. *Chem. Sci.* **2014**, *5*, 1463−1474.
(27) Nakashima, T.; Kajiki, Y.; Fukumoto, S.; Taguchi, M.; Nagao, S.; Hirota, S.; Kawai, T. *J. Am. Chem. Soc.* **2012**, *134*, 19877−19883.
(28) Hallett-Tapley, G. L.; D'Alfonso, C.; Pacioni, N. L.; McTiernan, C. D.; González-Béjar, M.; Lanzalunga, O.; Alarcon, E. I.; Scaiano, J. C. *Chem. Commun.* **2013**, *49*, 10073−10075.
(29) Simoncelli, S.; Aramendía, P. F. *Catal. Sci. Technol.* **2015**, *5*, 2110−2116.
(30) Titov, E.; Lysyakova, L.; Lomadze, N.; Kabashin, A. V.; Saalfrank, P.; Santer, S. *J. Phys. Chem. C* **2015**, *119*, 17369−17377.
(31) Bléger, D.; Schwarz, J.; Brouwer, A. M.; Hecht, S. *J. Am. Chem. Soc.* **2012**, *134*, 20597−20600.
(32) Knie, C.; Utecht, M.; Zhao, F.; Kulla, H.; Kovalenko, S.; Brouwer, A. M.; Saalfrank, P.; Hecht, S.; Bléger, D. *Chem. - Eur. J.* **2014**, *20*, 16492−16501.
(33) Boto, K. G.; Thomas, F. G. *Aust. J. Chem.* **1973**, *26*, 1251−1258.
(34) Studer, A.; Curran, D. P. *Nat. Chem.* **2014**, *6*, 765−773.
(35) Tong, X.; Pelletier, M.; Lasia, A.; Zhao, Y. *Angew. Chem., Int. Ed.* **2008**, *47*, 3596−3599.
(36) Enomoto, T.; Hagiwara, H.; Tryk, D. A.; Liu, Z. F.; Hashimoto, K.; Fujishima, A. *J. Phys. Chem. B* **1997**, *101*, 7422−7427.
(37) Alemani, M.; Peters, M. V.; Hecht, S.; Rieder, K. H.; Moresco, F.; Grill, L. *J. Am. Chem. Soc.* **2006**, *128*, 14446−14447.
(38) Dri, C.; Peters, M. V.; Schwarz, J.; Hecht, S.; Grill, L. *Nat. Nanotechnol.* **2008**, *3*, 649−653.
(39) Alemani, M.; Selvanathan, S.; Ample, F.; Peters, M. V.; Rieder, K. H.; Moresco, F.; Joachim, C.; Hecht, S.; Grill, L. *J. Phys. Chem. C* **2008**, *112*, 10509−10514.
(40) Moreno, J.; Gerecke, M.; Grubert, L.; Kovalenko, S. A.; Hecht, S. *Angew. Chem., Int. Ed.* **2016**, *55*, 1544−1547.
(41) You, Y.; Nam, W. *Chem. Soc. Rev.* **2012**, *41*, 7061.
(42) Xuan, J.; Xiao, W. *Angew. Chem., Int. Ed.* **2012**, *51*, 6828−6838.
(43) Prier, C. K.; Rankic, D. A.; MacMillan, D. W. C. *Chem. Rev.* **2013**, *113*, 5322−5363.
(44) Cismesia, M. A.; Yoon, T. P. *Chem. Sci.* **2015**, *6*, 5426−5434.
(45) Majima, T.; Tojo, S.; Ishida, A.; Takamuku, S. *J. Org. Chem.* **1996**, *61*, 7793−7800.
(46) Spreitzer, H.; Scholz, M.; Gescheidt, G.; Daub, J. *Liebigs Ann.* **1996**, *1996*, 2069−2077.
(47) Yeh, L. S. R.; Bard, A. J. *J. Electroanal. Chem. Interfacial Electrochem.* **1976**, *70*, 157−169.
(48) Yeh, L. R.; Bard, A. J. *J. Electroanal. Chem. Interfacial Electrochem.* **1977**, *81*, 333−338.
(49) Fox, M. A.; Hurst, J. R. *J. Am. Chem. Soc.* **1984**, *106*, 7626−7627.

DOI: 10.1021/jacs.6b10822
J. Am. Chem. Soc. 2017, 139, 335−341